

THE TEMPERATURE DEPENDENCE OF THE PARAMETERS OF NON-LINEAR STRESS-STRAIN RELATIONS FOR CARBON-EPOXY COMPOSITES

TEMPERATURNA ODVISNOST PARAMETROV NELINEARNE ODVISNOSTI NAPETOST-DEFORMACIJA ZA KOMPOZITE OGLJIKOVO VLAJKO-EPOKSI

Tomáš Kroupa, Robert Zemčík, Jan Klepáček

University of West Bohemia in Pilsen, Department of Mechanics, Univerzitní 22, 306 14, Plzeň, Czech Republic
kroupa@kme.zcu.cz

Prejem rokopisa – received: 2008-09-19; sprejem za objavo – accepted for publication: 2008-11-26

This work focuses on the identification of the parameters of stress-strain relations for a unidirectional, continuous-fiber carbon-epoxy composite under tensile loading at various temperatures. Simple tensile tests of thin strips with various fiber orientations were performed. The identification of the parameters for the chosen non-linear stress-strain relations is obtained at each temperature for which the experiment is performed and the strength is determined. The failure analysis for the determination of the first failure with the use of Puck's action-plane concept is performed, and the tensile and shear strength are investigated. The identification process with the use of a combination of the mathematical optimization method and a finite-element analysis is described with the necessary details. The temperature dependence of the parameters is also investigated.

Key words: composite, non-linear, carbon, epoxy, tensile, FEA, temperature

Cilj dela je bil identifikacija parametrov odvisnosti napetost-deformacija za enosmerne neprekinjene kompozite ogljikovo vlakno-epoksi pri natezni obremenitvi in pri različni temperaturi. Izvršeni so bili natezni preizkusi tankih trakov z različno orientacijo vlaken.

Za vsako temperaturo, pri kateri je bil preizkus izvršen, so bili identificirani parametri nelinearne odvisnosti napetost-deformacija, določene pa so bile tudi trdnosti. Analiza preloma s ciljem, da se določi začetek preloma, je bila izvršena z uporabo Puckovega koncepta o ploskvi delovanja in raziskani sta bili natezna in strižna trdnost. Opisan je proces matematične identifikacije in analize po metodi končnih elementov s potrebnimi detajli. Raziskana je bila tudi temperaturna odvisnost parametrov.

Ključne besede: kompozit, nelinearnost, ogljik, epoksi, natezen, FEA, temperatura

1 INTRODUCTION

The aim was to investigate the temperature dependence of the parameters of non-linear stress-strain relations for a unidirectional carbon-epoxy composite with the use of a finite-element (FE) analysis. The elasticity parameters and strengths were found from the comparison of the FE analysis and experimental results for simple tension tests of thin carbon-epoxy strips with dimensions 150 mm × 14.5 mm × 1.08 mm. Specimens with three fiber directions were used. The fiber directions formed angles of 0°, 45° and 90° with the direction of the loading force. The tensile tests were performed at 25 °C, 50 °C, 75 °C and 100 °C.

Two types of non-linear stress-strain relations are presented. Their capabilities for prediction of the behavior of the composite material loaded with simple tension at various temperatures were investigated. The strengths of the material were investigated with the use of Puck's failure criterion ⁵.

2 NON-LINEAR STRESS-STRAIN RELATIONS

Several types of stress-strain relations exist. A linear stress-strain relation is the simplest way to describe the

behavior of a composite material ². Unfortunately, it cannot describe the non-linear slope of the curves obtained from the tensile tests.

The next type is the non-linear stress-strain relation proposed in ¹, which takes into account a non-linear relationship between the shear stress and the strain only, and is generalized in ³. This relation can be written in a material axes coordination system L (longitudinal – fiber direction), T (transverse direction) for the state of plane stress in the form

$$\begin{bmatrix} \varepsilon_L \\ \varepsilon_T \\ \gamma_{LT} \end{bmatrix} = \begin{bmatrix} S_{11} & S_{12} & 0 \\ S_{21} & S_{22} & 0 \\ 0 & 0 & S_{66} \end{bmatrix} \begin{bmatrix} \sigma_L \\ \sigma_T \\ \tau_{LT} \end{bmatrix} + \begin{bmatrix} S_{111}\sigma_L & 0 & 0 \\ 0 & S_{222}\sigma_T & 0 \\ 0 & 0 & S_{6666}\sigma_{LT}^2 \end{bmatrix} \begin{bmatrix} \sigma_L \\ \sigma_T \\ \tau_{LT} \end{bmatrix} \quad (1)$$

where

$$S_{11} = \frac{1}{E_L} \quad (2)$$

$$S_{22} = \frac{1}{E_T} \quad (3)$$

$$S_{12} = -\frac{\nu_{LT}}{E_L} \quad (4)$$

$$S_{21} = -\frac{\nu_{TL}}{E_T} \tag{5}$$

$$S_{66} = \frac{1}{G_{LT}} \tag{6}$$

and

$$\nu_{TL} = \nu_{LT} \frac{E_T}{E_L} \tag{7}$$

The strains are expressed as polynomial functions of the stresses and the relation contains 7 independent parameters that can be sorted as linear parameters (Young's moduli) E_L, E_T, G_{LT} , Poisson's ratio ν_{LT} and the non-linear parameters S_{111}, S_{222} and S_{6666} . The orders of the polynomials are predetermined and suitable for the tests performed at normal temperatures. The whole relation (R1) has to be inverted for proper use in the FE software. The Newton iteration method is used in the work to find the roots of the equation

$$\mathbf{f}(\sigma_L, \sigma_T, \tau_{LT}) = \mathbf{S}\boldsymbol{\sigma} - \boldsymbol{\varepsilon} = \mathbf{0} \tag{8}$$

where \mathbf{S} is the stress-strain matrix, $\boldsymbol{\sigma}$ is the stress vector and $\boldsymbol{\varepsilon}$ is the strain vector.

The stress-strain relation, which takes into consideration the non-linear behavior of the composite material and where the stresses are explicit functions of strains, can be expressed in the form

$$\begin{bmatrix} \sigma_L \\ \sigma_T \\ \tau_{LT} \end{bmatrix} = \begin{bmatrix} \frac{E_L}{1-\nu_{LT}\nu_{TL}} & \frac{\nu_{LT}E_L}{1-\nu_{LT}\nu_{TL}} & 0 \\ \frac{\nu_{LT}E_L}{1-\nu_{LT}\nu_{TL}} & \frac{E_T}{1-\nu_{LT}\nu_{TL}} & 0 \\ 0 & 0 & G_{LT} \end{bmatrix} \begin{bmatrix} \varepsilon_L \\ \varepsilon_T \\ \gamma_{LT} \end{bmatrix} \tag{9}$$

where Ramberg-Osgood-based equations provide expressions for the tangent lamina stiffnesses

$$E_L = \frac{E_L^0}{\left[1 - \left(\frac{\varepsilon_L}{\varepsilon_L^0}\right)^{n_L}\right]^{1 + \frac{1}{n_L}}} \tag{10}$$

$$E_T = \frac{E_T^0}{\left[1 + \left(\frac{E_T^0 \varepsilon_T}{\sigma_T^0}\right)^{n_T}\right]^{1 + \frac{1}{n_T}}} \tag{11}$$

$$G_{LT} = \frac{G_{LT}^0}{\left[1 - \left(\frac{G_{LT}^0 \gamma_{LT}}{\tau_{LT}^0}\right)^{n_{LT}}\right]^{1 + \frac{1}{n_{LT}}}} \tag{12}$$

and the relation between the Poisson's ratios is considered as

$$\nu_{TL} = \nu_{LT} \frac{E_T^0}{E_L^0} \tag{13}$$

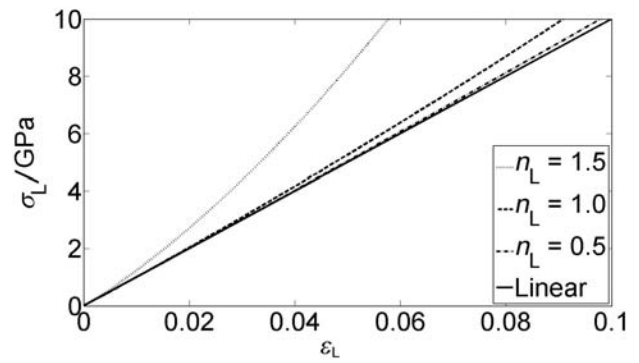


Figure 1: The influence of the shape parameter n_L
Slika 1: Vpliv parametrov oblike n_L

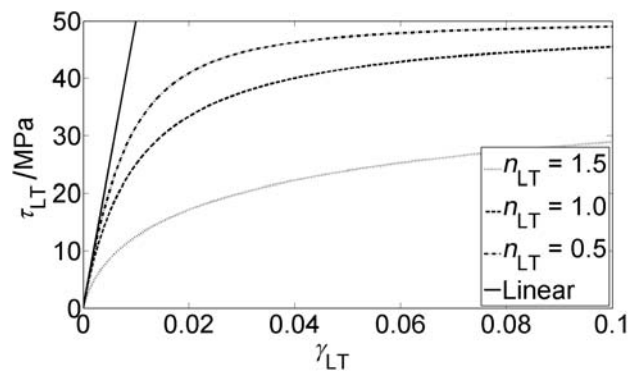


Figure 2: The influence of the shape parameter n_{LT}
Slika 2: Vpliv parametrov oblike n_{LT}

The relation (9) includes 10 independent parameters. These parameters are the initial moduli E_L^0, E_T^0, G_{LT}^0 , the asymptotic stress and strain levels σ_T^0, τ_{LT}^0 and ε_L^0 , the shape parameters n_L, n_T, n_{LT} and the Poisson's ratio ν_{LT} . Figure 1 shows the influence of the shape parameter n_L for a material with $E_L^0 = 100$ GPa and $\varepsilon_L^0 = 1$.

Figure 2 shows the influence of the shape parameter n_{LT} for the material with $G_{LT}^0 = 5$ GPa and $\tau_{LT}^0 = 50$ MPa.

3 IDENTIFICATION OF THE ELASTICITY PARAMETERS

The identification of the elasticity parameters is the first step in the identification process. The method used for the identification of the elasticity parameters, which combines the material axis and the off-axis tensile tests, the FE analysis and the mathematical optimization method will be described in the following paragraph.

Non-linear stress-strain relations have to be implemented into the FE software first. The number of elements in the FE models for the calculation of the force-displacement diagrams has to be reduced as much as possible. The reduction of the number of elements is necessary for the reduction of the time consumption during the optimization cycles. The next step is to propose the residual function that represents the difference between the numerical and the experimental

results at the given optimization step, and which is minimized. The function is proposed as

$$r = \sum_{\theta} \frac{\sum_p [F_{exp}(\theta, p) - F_{num}(\theta, p)]^2}{\max_p [F_{exp}(\theta, p)]} \quad (14)$$

where θ is the fiber angle, $r(\theta)$ is the residual of the force-displacement diagram for the fiber angle θ , which had values $0^\circ, 15^\circ, 30^\circ, 45^\circ, 60^\circ, 75^\circ$ and 90° ; p is the displacement where the residual is calculated; $F_{num}(\theta, p)$ is the calculated force corresponding to the displacement p of the strip with the fiber angle θ ; $F_{exp}(\theta, p)$ is the experimentally measured force corresponding to the displacement p of the strip with the fiber angle θ and $\max_p [F_{exp}(\theta, p)]$ is the maximum force measured as a response of the strip with a fiber angle θ , used as a normalization coefficient.

It should be noted that the Poisson's ratio ν_{LT} has to be identified with a special, separate test and, therefore, it will not be investigated in this paper, and its value is taken as $\nu_{LT} = 0.28$. The tests, probably a biaxial test able to precisely describe the potential strain dependence of the Poisson's ν_{LT} ratio, and a further analysis of the influence of the temperature on the Poisson's ratio ν_{LT} will be performed in the near future.

The flow chart of the whole automated process of the identification of the elasticity parameters is shown in **Figure 3**.

4 IDENTIFICATION OF THE STRENGTHS

Once the elasticity parameters are identified, the identification of the strengths can be performed. The failure criterion used in the strengths identification process is Puck's action-plane concept. For more about

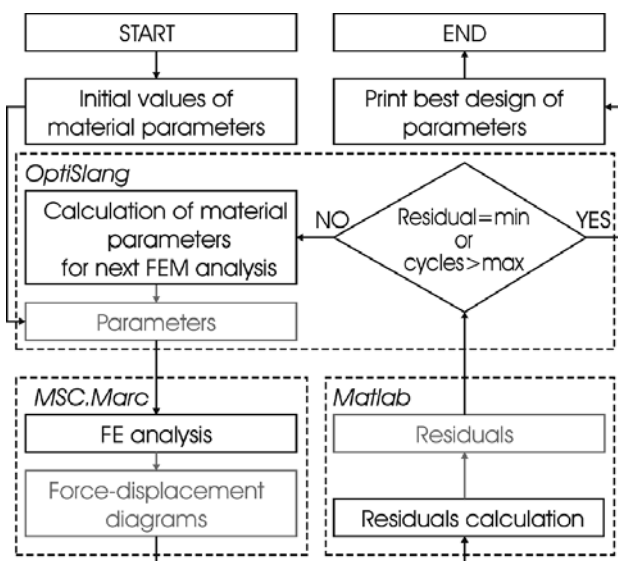


Figure 3: Identification process of the elasticity parameters
Slika 3: Proces identifikacije parametara elastičnosti

the criterion, see ⁴⁻⁶. Once the tensile test is performed, only the tensile X^T, Y^T and the shear S^L strengths can be identified. The identification of the strengths is performed with the use of a minimized function, which is proposed as the sum of the errors between the average of the measured ultimate forces and the calculated ultimate force for each fiber angle

$$r = \sum_{\theta} [F_{exp}^u(\theta) - F_{num}^u(\theta)] \quad (15)$$

where θ is the fiber angle, $F_{exp}^u(\theta)$ is the average of the measured ultimate forces for the given fiber angle θ and $F_{num}^u(\theta)$ is the calculated ultimate force for the given fiber angle θ . The flow chart of the identification process of the strengths is shown in **Figure 4**.

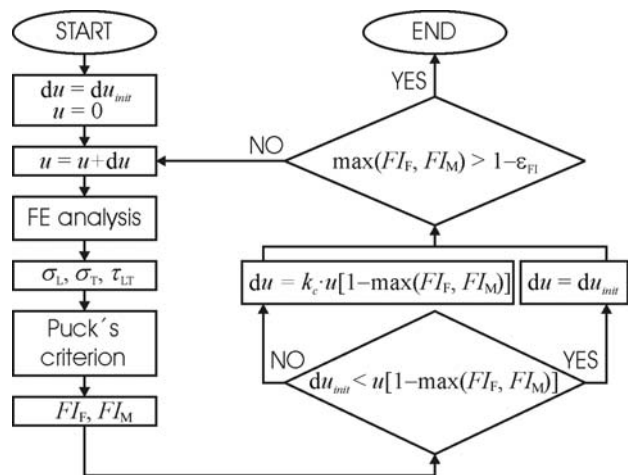


Figure 4: Identification process of the strengths
Slika 4: Proces identifikacije trdnosti

Let us briefly describe the flow chart in **Figure 4**. At the start of the identification process the initial displacement increment du_{mit} is prescribed. The FE analysis is the next step. Subsequently, the failure analysis is performed and the failure indices (FIs) are calculated. These indices represent the level of the load with respect to the strength of the material. If the FI reaches one, the material is damaged. Once the FIs are calculated, the decision process that results in the displacement increment that is applied in the next step is performed. The constant k_c is used to improve the convergence speed. Once the matrix-failure index FI_M or the fiber-failure index FI_F reaches 1 (with the toleration ϵ_{FI}) the identification process ends.

5 RESULTS

The identified elasticity parameters using the relationship (1) are shown in **Table 1**.

The decreasing tendency of the linear parameters and the increasing tendency of the non-linear part of the parameters with increasing temperature are evident. The exceptions are the shear modulus, which increases with the temperature $100^\circ C$, and the Young's modulus for the fiber direction E_L , which remains constant.

Table 1: Elasticity parameters used in (1)

Tabela 1: Parametri elastičnosti uporabljeni v (1)

Parameter	25 °C	50 °C	75 °C	100 °C
E_L /GPa	111.58	111.69	111.47	111.59
E_T /GPa	8.48	7.30	6.50	4.77
G_{LT} /GPa	3.98	4.10	3.83	8.69
$(S_{111} \cdot 10^{-22})/\text{Pa}^{-2}$	-4.66	-4.67	-4.65	-4.49
$(S_{222} \cdot 10^{-19})/\text{Pa}^{-2}$	3.46	3.78	5.79	68.47
$(S_{666} \cdot 10^{-26})/\text{Pa}^{-3}$	12.75	21.97	58.93	442.27

Table 2 shows the identified parameters that were obtained by using relation (9).

Table 2: Elasticity parameters used in (9)

Tabela 2: Parametri elastičnosti uporabljeni v (9)

Parameter	25 °C	50 °C	75 °C	100 °C
E_L^0 /GPa	106.26	107.71	106.19	107.51
E_T^0 /GPa	8.25	7.15	6.38	4.35
G_{LT}^0 /GPa	3.44	3.27	3.00	2.34
ϵ_L^0	1.44	0.72	1.49	0.78
σ_T^0 /MPa	176.52	147.00	129.52	33.64
τ_{LT}^0 /MPa	56.66	38.80	31.48	17.28
n_L	0.56	0.65	0.56	0.64
n_T	1.38	1.61	1.35	1.33
n_{LT}	1.44	1.83	1.53	1.89

The initial Young's modulus in the fiber direction is constant, while the rest of the initial moduli show a decreasing tendency. The asymptotic strain level does not show any dependence on the temperature. The asymptotic stress levels decrease with the increasing temperature. The values of the shape parameters are oscillating. **Figure 5** shows the temperature dependence of the residual (14). The increase of the residuals of the relation (1) with the increase of the temperature is obvious and the better capability of relation (9) is evident.

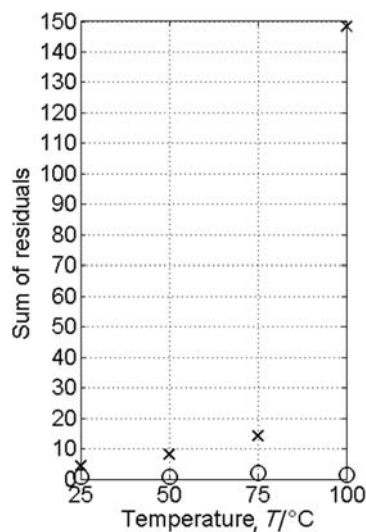


Figure 5: Sum of the residuals calculated with the use of (14) (x – (1), o – (9))

Slika 5: Vsota rezidualov, izračunana s uporabo (14) (x – (1), o – (9))

Table 3: Strength identified with the use of (1)

Tabela 3: Trdnosti določene z uporabo (1)

Strength	25 °C	50 °C	75 °C	100 °C
X^T /MPa	1937.2	1937.0	1937.1	1937.0
Y^T /MPa	36.7	38.2	32.8	16.9
S^L /MPa	58.4	49.3	39.2	73.6

Table 4: Strengths identified with the use of (9)

Tabela 4: Trdnosti izračunane z uporabo (9)

Strength	25 °C	50 °C	75 °C	100 °C
X^T /MPa	1937.0	1937.0	1937.1	1937.0
Y^T /MPa	36.4	38.2	32.8	16.9
S^L /MPa	61.0	49.3	39.2	73.6

The temperature independence of the strength X^T is visible from **Tables 3 and 4**. Also, the decreasing tendency of the strength Y^T and S^T is evident, except for the high value of the shear strength for 100 °C. The differences between the sums of the errors between the ultimate forces are negligible.

6 CONCLUSION

The capabilities of two types of non-linear stress-strain relations were investigated. The better suitability of the stress-strain relation based on the Ramberg-Osgood equations was proven. The influence of the viscoelasticity was neglected in the work.

The Puck's failure criterion was used for the failure analysis and the prediction of the strengths. It provides acceptable results for temperatures up to 75 °C.

Acknowledgements

The work has been supported by the research project of the Ministry of Education of the Czech Republic no. MSM 4977751303 and the project of the Grant Agency of the Czech Republic GACR no. 101/07/P059.

7 REFERENCES

- H. T. Hahn, W. S. Tsai, Nonlinear elastic behavior of unidirectional composite laminae, *Journal of Composite Materials*, 7 (1973), 102–118
- J. M. Berthelot, *Composite materials*, Springer, New York 2004, p. 639
- F. Hassani, M. Shokrieh, L. Lessard, A fully non-linear 3-D constitutive relationship for the stress analysis of a pin loaded composite laminate, *Composites Science and Technology*, vol. 62 (2002) 3, 429–439
- T. Kroupa, V. Laš, Off-axis behavior of unidirectional FRP composite, *Mater. Technol.* 42 (2007) 3, 125–129
- A. Puck, H. Schürmann, Failure analysis of FRP laminates by means of physically based phenomenological models. *Composites Science and Technology*, vol. 58 (1998) 7, 1045–1067
- V. Laš, R. Zemčík, Progressive Damage of Unidirectional Composite Panels, *Journal of Composite Materials* 42 (2008), 25–44